Two-photon selective reflection

M. Gorris-Neveux, P. Monnot, S. Saltiel,* R. Barbé, J.-C. Keller,[†] and M. Ducloy

Laboratoire de Physique des Lasers, URA CNRS 282, Institut Galilée, Université Paris-Nord, 93430 Villetaneuse, France

(Received 21 March 1996)

The conditions of observation of *direct* two-photon-induced dispersion in three-level reflection spectroscopy at a vapor-dielectric interface are discussed. One shows how *pump frequency modulation* allows one to discriminate the two-photon singular contribution associated with atoms moving quasiparallel to the dielectric interface, and therefore single out off-resonant Doppler-free two-photon dispersion in selective reflection. A nonperturbative theoretical approach to two-photon reflection is shown to predict a dynamic Stark shift of the two-photon resonance, which has been experimentally observed on the $6S$-$6P$-$8S$ transition of cesium. [S1050-2947(96)06009-X]

PACS number(s): 42.65.−k, 32.80.Wr, 42.25.Gy

I. INTRODUCTION

Selective reflection [1] has recently regained interest since it has been shown that it can exhibit sub-Doppler features, when the reflection of light is monitored at *normal incidence* on the interface between a dielectric window and a *low-density vapor* [2]. In particular, frequency-modulated selective reflection has been demonstrated as a powerful means of monitoring long-range interactions between excited atoms and solid-state surfaces [3,4].

Nonlinear selective reflection spectroscopy in *cascade-up three-level* systems has been studied recently both theoretically [5] and experimentally [6,7]. The modification of the refractive index of a vapor, induced by a pump beam (resonant with a transparent atomic transition between two excited states) has been demonstrated on cesium vapor [6,7] by monitoring the reflectivity change of a probe beam tuned to the resonance transition (Fig. 1). Two beam geometries at the interface are usually considered: either copropagating or counterpropagating beams, as shown on Fig. 2. The attractive feature of this pump-probe three-level selective reflection spectroscopy is that, by choosing copropagating or counterpropagating geometry, one can excite and detect selectively atoms departing from or arriving at the surface, as shown in Ref. [6].

In the previous investigations, the pump power was, in general, kept relatively low in order to allow for the interpretation of the experimental observations in the framework of a third-order theoretical approach. On the other hand, one expects that, at high pump power, similar effects to that observable in three-level transmission spectroscopy [8] should take place. However, saturation effects in selective reflection spectroscopy (line broadening and shift, line splitting, etc.) may differ because, besides the steady-state atomic response similar to that monitored in transmission spectroscopy, there is also a transient response associated with the atoms leaving the interface.

In the present paper, we describe a theoretical and experimental investigation of two-photon selective reflection at arbitrary pump power. We show that, as a result of increasing pump powers: (i) the *stepwise* coherent three-level resonance (observable when pump frequency is blue detuned [6]) broadens and splits, and (ii) the *direct* two-photon resonance (observable when pump frequency is red detuned) is blue-shifted. The experimental investigation of this process was performed with the $6S_{1/2}(F=4) \Rightarrow 6P_{3/2}(F'=5) \Rightarrow 8S_{1/2}(F''=4)$ coupled transitions of Cs and in a counterpropagating beam geometry.

II. THEORETICAL CONSIDERATIONS

A. Basic equations

The theoretical analysis of three-level selective reflection, presented in Ref. [5], is extended in the following, in two aspects: (i) pump frequency modulation will be included, and (ii) arbitrary pump power will be considered. At normal incidence, the probe reflection coefficient is given by

$$R = \left(\frac{n-1}{n+1}\right)^2 + \frac{4n(n-1)}{(n+1)^3} \, \text{Re} \, T, \qquad (1)$$
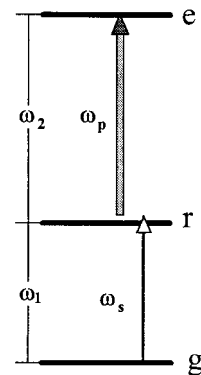
FIG. 1. Cascade three-level system. The pump beam with frequency ω_p is resonant with the upper transition (resonance frequency ω_2), while the probe beam with frequency ω_s is resonant with the lower transition (resonance frequency ω_1).

*Permanent address: Physics Department, University of Sofia, 1164 Sofia, Bulgaria.

[†]FAX: 33-1-49 40 32 00. Electronic address: KELLER@LPL.UNIV-PARIS13.FR

where

$$\text{Re}T = -\text{Re}\frac{\hbar N\Omega_s}{4\varepsilon_0 E_s^2}\left[\int_{-\infty}^0 dv\ W(v)\bar{\sigma}_{rg}(v) + \int_0^\infty dv\, W(v)(-2ik_s)\hat{\sigma}_{rg}(-2ik_s,v)\right]. \tag{2}$$

In this expression $\hat{\sigma}_{rg}(-2ik_s,v)$ is the Laplace transform of the time-dependent matrix element of the reduced density operator σ (see Ref. [5] for more details):

$$\hat{\sigma}_{rg}(-2ik_s,v) = -\frac{\Omega_s}{4k_s}\frac{A_2/2 - i\Delta + i(k_p - k_s)v}{[A_2/2 - i\Delta + i(k_p - k_s)v](A_1/2 - i\Delta_s - ik_s v) + \Omega_p^2/4}, \tag{3}$$

where Ω_s and Ω_p are the probe and pump Rabi frequencies, respectively ($\Omega_s = 2\mu_{rg}E_s/\hbar$, $\Omega_p = 2\mu_{er}E_p/\hbar$), k_s and k_p are pump and probe wave numbers (k_s is positive; the sign of k_p depends on beam geometry). $\Delta_p = \omega_p - \omega_2$ and $\Delta_s = \omega_s - \omega_1$ are the detunings of the pump and the probe frequency from the exact resonances of the upper and lower transitions, and $\Delta = \Delta_s + \Delta_p$ is the two-photon detuning. $W(v)$ is the normalized velocity distribution (v is velocity normal to the surface). The probe and pump fields are denoted with E_s and E_p. N is the atomic density, and n the index of refraction of the glass. A_1 and A_2 are the total decay rates of the intermediate level r and of the excited level e, respectively.

In Eq. (2) $\bar{\sigma}_{rg}(v)$ is the stationary value for the reduced density matrix:

$$\bar{\sigma}_{rg}(v) = \frac{i\Omega_s}{2}\frac{A_2/2 - i\Delta + i(k_p + k_s)v}{[A_2/2 - i\Delta + i(k_p + k_s)v](A_1/2 - i\Delta_s + ik_s v) + \Omega_p^2/4}. \tag{4}$$

Such selective reflection spectra as that described by Eq. (2) may be monitored via amplitude modulation of the pump [6,7]. As shown in [5] for low intensities of the pump and probe, and when $k_s/|k_p| < 1$, the spectra consist of three types of resonances: one that corresponds to the stepwise velocity selective coherent resonance (SVS) at position $\Delta_s = -(k_s/|k_p|)\Delta_p$, which exists only for $\Delta_p > 0$, a second one at $\Delta_s = 0$ (probe resonance), and a third one that corresponds to the direct $(g \to e)$ two-photon coherent resonance (DTP) at position $\Delta_s = -\Delta_p$. The weak DTP is generaly masked by the other resonances.

To enhance the DTP contrast we consider in the following the effect of pump frequency modulation (FM) on the probe reflectivity [4,9]. With this technique, the central resonance at $\Delta_s = 0$ is reduced since its position does not depend on pump frequency. In the FM mode, the amplitude modulation induced on the probe reflection, I_{FM}, is proportional to $(d\,\text{Re}\,T)/d\omega_p$. With the assumption of a Maxwell-Boltzmann velocity distribution, the reflection signal is given by

$$I_{\text{FM}} = B\frac{4n(n-1)}{(n+1)^3}\frac{d\,\text{Re}T}{d\omega_p}I_s$$

i.e.,

$$I_{\text{FM}} = -B\frac{4n(n-1)}{(n+1)^3}\frac{N\hbar c\Omega_s^2\Omega_p^2}{32v_0\sqrt{\pi}}\text{Re}(J_+ + J_-), \tag{5}$$

where
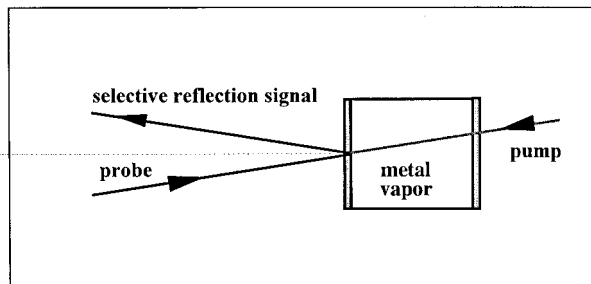
FIG. 2. Counterpropagating geometry of interaction of pump and probe beam at the glass-metal vapor interface.

$$J_\pm = \int_0^\infty dv\ \exp\left(-\frac{v^2}{v_0^2}\right)\left\{\left[\frac{A_2}{2} - i\Delta - ik_s v s_\pm\right]\right.$$
$$\left.\times\left(\frac{A_1}{2} - i\Delta_s - ik_s v\right) + \frac{\Omega_p^2}{4}\right\}^{-2}, \tag{6}$$

with $s_\pm = (1 \mp k_p/k_s)$, B a constant proportional to the depth of frequency modulation, and I_s the intensity of the probe beam ($I_s = \varepsilon_0 c|E_s|^2$).

The notations J_+ and J_- have definite physical meaning. J_+ represents the (transient) contribution of atoms with positive velocities (departing atoms) and J_- represents the (steady state) contribution of atoms with negative velocities (arriving atoms).

Expressions (5) and (6) are valid for both copropagation and counterpropagation geometries. For copropagating geometry, $k_p > 0$ and for counterpropagating geometry, $k_p < 0$. It is seen from (6) that, because of the relations

$$J_+(k_p > 0) = J_-(k_p < 0)\quad\text{and}\quad J_-(k_p > 0) = J_+(k_p < 0)$$

valid for symmetrical velocity distributions, the contribution of the arriving atoms in the spectra obtained with copropagation geometry is the same as the contribution of the departing atoms in the spectra obtained with counterpropaga-
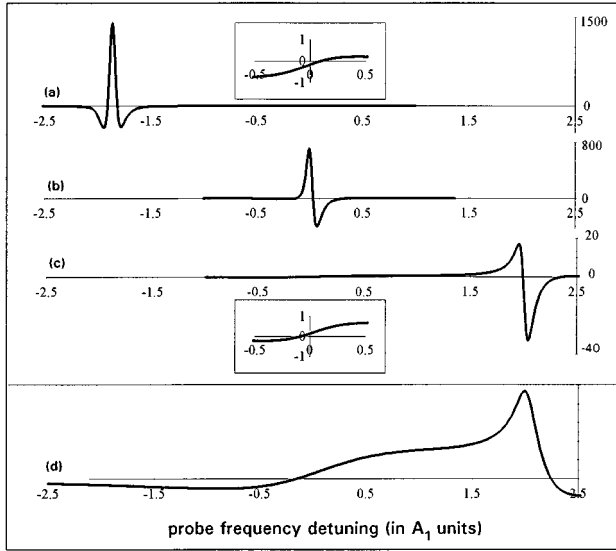
FIG. 3. Spectral variations of the pump-induced probe reflectivity for frequency modulation of the pump and in the nonsaturated regime, calculated with analytical formula from the Appendix. Pump detuning is positive ($\Delta_p = 2A_1$) in (a), zero in (b), and negative ($\Delta_p = -2A_1$) in (c). Vertical scale is $\mathrm{Re}(\widetilde{J}_+ + \widetilde{J}_-)$ (see the Appendix). For all spectra $A_2/A_1 = 0.1$, $k_s/|k_p| = 0.93$, $\Omega_p = 0.001A_1$. The spectrum (d) is calculated for the same parameters as (c), but with amplitude modulation of the pump.

tion geometry. And also the contribution of the departing atoms in the spectra obtained with copropagation geometry is the same as the contribution of the arriving atoms in the spectra obtained with counterpropagation geometry. For this reason, in the case of symmetrical velocity distributions, the spectra for the two geometries should be identical.

In the Doppler limit, when $|\Delta_p|, |\Delta_s| \ll k_s v_0$ (v_0 is the average thermal velocity of the atoms) the integral (6) can be solved analytically, as shown in the Appendix. In the case of arbitrary pump detunings Δ_p, this formula can be integrated only numerically. In Fig. 3 are shown the line shapes of the FM reflection resonances for three different values of the detuning Δ_p. For positive Δ_p, the spectra consist of a strong SVS resonance at position $\Delta_s = -(k_s/k_p)\Delta_p$. It has an absorptionlike form and a width that does not depend on the value of Δ_p. In the nonsaturating regime, when $\Omega_p < A_2$, the distance between the two minima is $\gamma_{\mathrm{SVS}} = [k_s/|k_p|A_2 + (1-k_s/|k_p|)A_1]$. The line shape of the "$\Delta_s = 0$" resonance depends on the value of Δ_p. For $\Delta_p \cong 0$ it has relatively high amplitude and dispersionlike shape [Fig. 3(b)]. For $\Delta_p \neq 0$ it has an inverted dispersionlike shape [see the insets on Figs. 3(a) and 3(c)] and is very weak with respect to the other resonances as should be expected when frequency modulation of the pump is used.

For negative Δ_p the spectra consist of a DTP resonance at position $\Delta_s \cong -\Delta_p$ [see Fig. 3(c)]. It has dispersionlike form for small values of A_2/A_1 and an absorptionlike form for $A_2/A_1 \cong 1$ as shown in Fig. 4. This DTP resonance is related to *off-resonant Doppler-free two-photon dispersion* of the vapor. As in linear selective reflection [2–4], there is a singular sub-Doppler contribution to the two-photon reflection associated mostly with *atoms moving parallel to the surface*, and satisfying the resonance condition $\omega_s + \omega_p = \omega_1 + \omega_2$ (see
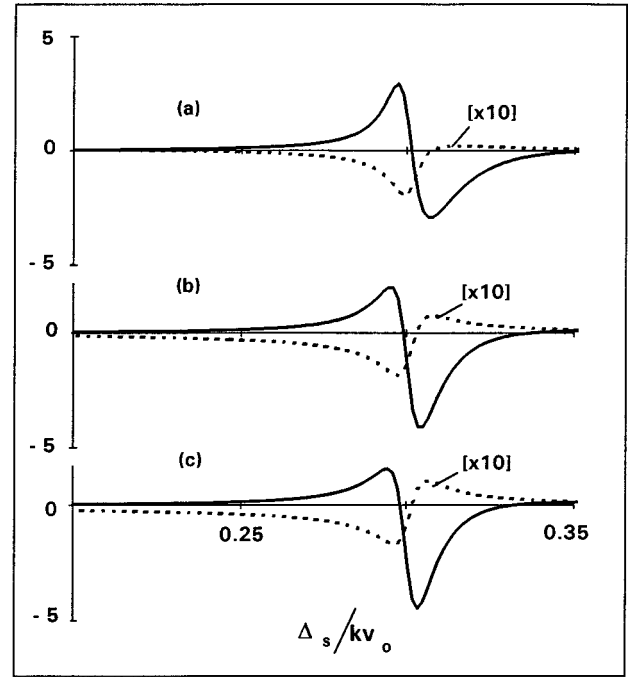
FIG. 4. Theoretical line shapes (solid line) of the direct two-photon resonance for different values of the A_2/A_1 parameter: (a) $A_2/A_1 = 1/30$; (b) 1/10, and (c) 1/3. For all spectra $A_2 = 0.01kv_0$, $k_s/|k_p| = 0.93$, $\Omega_p = 0.001kv_o$. The solid line yields the predicted line shape $[\propto \mathrm{Re}(J_+ + J_-)]$ while the dashed line shows the contribution of departing atoms $[\propto \mathrm{Re}(J_+)]$ (in the case of a counter-propagating geometry).

Fig. 1). The amplitude of this resonance drops very quickly with increasing pump detuning Δ_p, and for large Δ_p it decreases as $1/\Delta_p^2$ as expected in two-photon spectroscopy [10]. This frequency dependence is related to the homogeneous *Lorentzian* part of the atomic response, and should be compared with that of the SVS resonance in which resonant velocity selection is responsible for a *Gaussian* frequency dependence such as $W(v_{\mathrm{SVS}})$ with $v_{\mathrm{SVS}} = \Delta_p/k_p$.

Far off resonance, when $|\Delta_p| \gg k_s v_0$, we can find an analytical expression for the shape of the DTP resonance. Indeed, in this case, Eq. (6) can be approximated as

$$J_\pm = \frac{1}{\Delta_s^2} \int_0^\infty \left[\left(i\frac{A_2}{2} + \Delta - \frac{\Omega_p^2}{4\Delta_s} \right) + k_s v s_\pm \right]^{-2}$$
$$\times \exp\left(-\frac{v^2}{v_0^2} \right) dv. \tag{7}$$

The amplitude I_{DTP} of the DTP peak (for $A_2 \ll |k_s v_0 s_\pm|$) will be

$$I_{\mathrm{DTP}} = -B\,\frac{4n(n-1)}{(n+1)^3}\,\frac{N\hbar c\Omega_s^2\Omega_p^2}{32k_s v_0 \sqrt{\pi}}\,\frac{1}{\Delta_p^2}$$
$$\times \frac{\Delta - \Omega_p^2/4\Delta_s}{(\Delta - \Omega_p^2/4\Delta_s)^2 + A_2^2/4}\left[\frac{1}{s_+} + \frac{1}{s_-} \right]. \tag{8}$$

From Eq. (8) it can be seen that the two-photon reflection signal is the sum of two terms, $1/s_\pm$; each of them has a
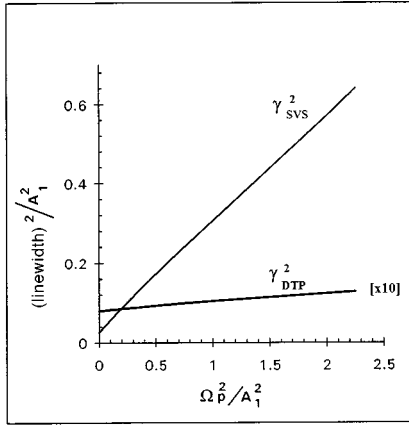
FIG. 5. Theoretical predictions for the variations of the square of the linewidth of the three-level resonances as a function of the square of the pump Rabi frequency. Pump detuning is $\Delta_p = 3A_1$ for the γ^2_{SVS} dependence and $\Delta_p = -3A_1$ for the γ^2_{DTP} dependence. The parameters of the three-level system are $A_2/A_1 = 0.1$ and $k_s/|k_p| = 0.93$.

dispersive form but reversed because s_+ and s_- have opposite signs (if $|k_p| > k_s$). The first of these terms reflects the contribution of the departing atoms, and the second reflects that of the arriving atoms. For a counterpropagation scheme and for the ratio $k_s/|k_p| = 0.93$, the contribution of the arriving atoms $(1/s_-)$ is 30 times bigger than the contribution of the departing atoms $(1/s_+)$. This difference in size is related to the effective two-photon Doppler shift, $k_s v s_\pm$. As can be deduced from Eq. (7), the width of the velocity group contributing to the two-photon resonance is determined by $k_s v s_\pm \lesssim A_2$, and, as a consequence, the size of the contribution is inversely proportional to the two-photon Doppler broadening, $\Delta v/v_0 \cong A_2/k_s v_0 s_\pm$. The line center is situated at $\Delta_s = -\Delta_p + \Omega_p^2/4\Delta_s$ so that, in this approximation, the two-photon resonance is blueshifted by $\Omega_p^2/4\Delta_s$. According to this simple model, the width of the curve does not depend on the pump intensity and on the detuning Δ_p, and is equal to A_2 (compare with the dependence shown in Fig. 5). Let us recall that, in the experiments with pump amplitude modulation, the width of this two-photon coherent peak is proportional to $\sqrt{A_2|\Delta_p|}$ and, because of that, it is difficult to monitor it at large values of Δ_p. In Figs. 3(c) and 3(d) we compare two-photon selective reflection spectra obtained with amplitude modulation of the pump and with frequency modulation of the pump. The advantage of the FM approach is evident.

B. Pump saturation effects

Several saturation effects can be seen in the spectra when $\Omega_p > A_2$. The reflection resonances broaden with increasing Ω_p, as shown on Fig. 5. The change of the square of the width of the SVS and DTP resonances depends linearly on the pump intensity, and can be fitted by the following relations:

$$\gamma^2_{\text{SVS}} = \left[\frac{k_s}{k_p} A_2 + \left(1 - \frac{k_s}{k_p} \right) A_1 \right]^2 + 0.3\Omega_p^2, \qquad (9)$$
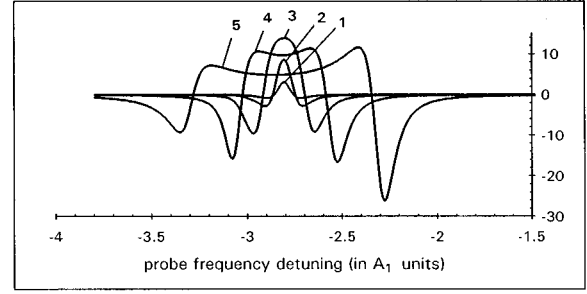
FIG. 6. Theoretical spectra for SVS line shape for saturating pump. Pump Rabi frequencies are as follow: $\Omega_p/A_1 = 0.1$ (1), 0.2 (2), 0.5 (3), 1 (4), and 2 (5). The parameters of the three-level system are $A_2/A_1 = 0.1$ and $k_s/|k_p| = 0.93$.

$$\gamma^2_{\text{DTP}} = (0.9A_2)^2 + 0.027\Omega_p^2. \qquad (10)$$

We have checked that the coefficient 0.3 in front of Ω_p^2 in the formula (9) does not depend on the ratio A_2/A_1. We will use formula (9) in the experimental part for determination of the effective Ω_p. At pump intensity for which the corresponding Rabi frequency is larger than A_1, the SVS resonance exhibits dynamic Stark splitting (Fig. 6) as in three-level transmission spectroscopy [8].

Another pump saturation effect is the pump-induced blueshift of the DTP resonance predicted for red detunings of the pump frequency. The shift depends almost linearly on the pump intensity. In Fig. 7 are compared the theoretical shift as a function of the square of the Rabi frequency of the pump obtained either by the simple approach (8), or by the analytical formula from the Appendix, or by the numerical integration (5) and (6). One notes perfect agreement between the predictions obtained with the analytical formula and the numerical integration approach. Because of that, most of the theoretical graphs shown in the paper have been obtained with the analytical formula (A5).
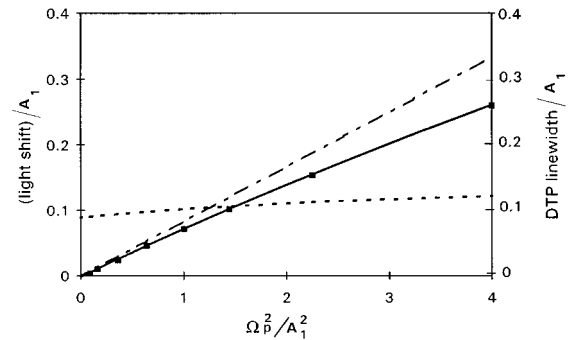
FIG. 7. Dynamic Stark shift of the DTP resonance ($\Delta_p = -3A_1$) as a function of the square of the pump Rabi frequency. Three models are compared: the dashed-dotted line is the shift predicted by Eq. (8), the solid line is the shift obtained with the analytical formula from the Appendix [Eq. (A5)], and the squares are the shift obtained with the numerical integration [Eq. (5)]. The dotted line yields the broadening of the DTP resonance. The light shift gets larger than the DTP linewidth for $\Omega_p/A_1 > 1.2$.
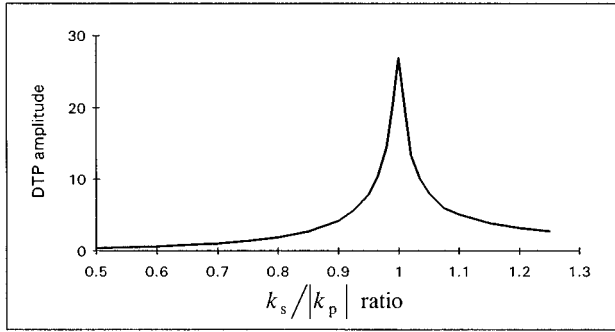
FIG. 8. Theoretical dependence of the DTP amplitude ($\Delta_p = -0.3kv_0$) on the ratio $k_s/|k_p|$ obtained with Eq. (5) for non-saturating pump intensities ($\Omega_p = 0.001kv_0$). The parameters of the three-level system are $A_2/A_1 = 0.1$ and $A_1/kv_0 = 0.1$.

C. The role of the $k_s/|k_p|$ parameter

The amplitude of the DTP resonance depends strongly on the ratio of $k_s/|k_p|$. The closer this ratio is to one, the higher the amplitude of the DTP resonance (Fig. 8). Taking these results into account, we choose for the experiment in Cs vapor a three-level system with the parameter $k_s/|k_p|$ close to 1. In the case of $k_s/|k_p| > 1$ the two-photon spectra are different. The SVS is no longer present (as in transmission spectroscopy [8]) and the DTP resonance at $\Delta_s = -\Delta_p$ should be observable independently of the sign of Δ_p. For $\Delta_p > 0$ (i.e., $\Delta_s < 0$) the two-photon resonance is redshifted as expected from Eq. (8). The line shape of the DTP resonances is identical on both sides of the central resonance, but with a change of sign.

III. EXPERIMENT

A. Experimental setup

Two-photon selective reflection experiments have been performed on a $6S_{1/2}(F=4) \Rightarrow 6P_{3/2}(F'=5) \Rightarrow 8S_{1/2}(F''=4)$ cascade transition of Cs (Fig. 9): the first transition is the resonance line at 852 nm, the second one is at 795 nm. The parameter $k_s/|k_p|$ for this cascade transition is 0.9323. The spontaneous decay rates are $A_1 = 5.3$ MHz for $6P_{3/2}$ and $A_2 = 1.8$ MHz for $8S_{1/2}$ [11]. The hyperfine structure of all three levels was resolved in our experiment and we were able to spectrally select the levels indicated in the figure.
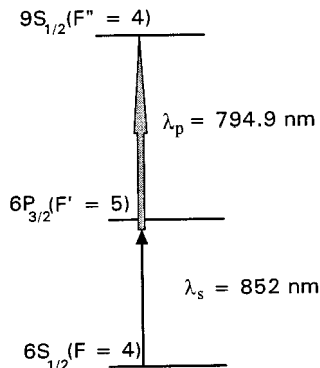
FIG. 9. Cesium $6S$-$6P$-$8S$ cascade transitions used in the experiments with the relevant sublevels.
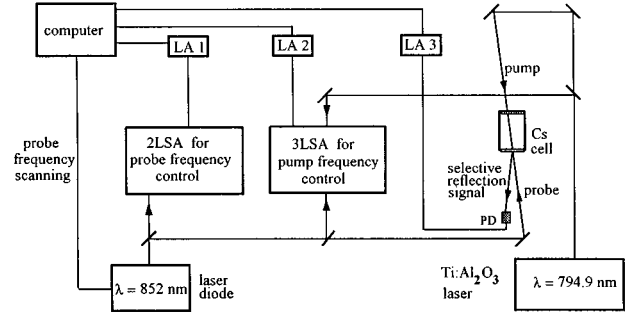
FIG. 10. Experimental setup: LA1, LA2, LA3: lock-in amplifiers; 2LSA: two-level saturated absorption setup; 3LSA: three-level saturated absorption setup.

The lower transition was excited by a frequency-stabilized laser diode with a typical 10-mW output power at 852 nm. The diode cavity is coupled via a weak optical feed-back to an external confocal Fabry-Pérot cavity in order to reduce the laser jitter well below 1 MHz [12]. The pump beam is provided by a single-mode ring cavity titanium sapphire laser pumped by a 10 W argon laser. The output of the Ti:Al$_2$O$_3$ laser is stabilised to a reference cavity with the simple fringe-locking technique and a piezocontrolled mirror as compensating element [13]. The output of the laser can be tuned in the range 720–800 nm with maximum power 500 mW; its jitter is less than 1 MHz.

In the experimental investigation of the two-photon selective reflection, we used COUNTERPROPAGATING geometry shown in Fig. 2. Overlapping probe and pump beams are incident at small angle (5 mrad) on the interface between a dielectric window (glass) and the Cs vapor. We study the modification of the reflection coefficient of the probe beam induced by the presence of the pump beam. This contribution is isolated from the main part of the reflection coefficient by pump frequency modulation techniques. Pump FM induces amplitude modulation of the reflected probe beam that is monitored by a lock-in amplifier (Fig. 10). In all experiments, the probe frequency is scanned continuously over the hyperfine transitions of the cesium D_2 resonance line, while the pump frequency is fixed and quasiresonant with the upper transition. Several probe reflection spectra can thus be recorded with the pump frequency changed step by step.

For absolute frequency reference of both pump and probe frequency two side setups are used: two-level saturated absorption (2LSA) for probe frequency control and three-level saturated absorption (3LSA) for pump frequency control. This calibration technique is described in detail in [6,7].

The complete experimental scheme is shown in Fig. 10. The three spectra (the two reference and the reflection spectra) are detected simultaneously and the data are memorized with the computer, which controls the laser diode frequency scanning. The diameters of the beams are 3 mm for the probe beam and 5 mm for the pump one. Their intensity can be changed continuously with variable attenuators up to 2 mW for the probe beam and to 200 mW for the pump beam. All spectra were taken at low probe intensity (~ 0.7 mW/cm^2) in order to avoid probe saturation effects. Pump intensities were much higher—from 50 to 1000 mW/cm^2.
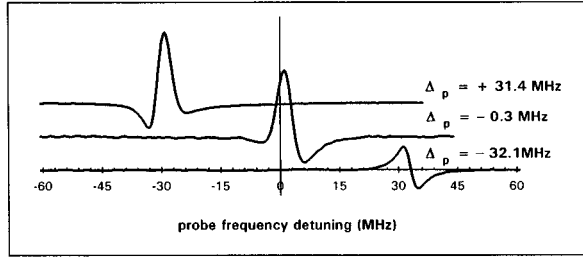
FIG. 11. Three-level selective reflection spectra for different values of pump frequency detuning Δ_p. Pump intensity: 0.25 W/cm^2. Vertical scale is in arbitrary units (identical for all measurements).

B. Three-level selective reflection spectra

Three-level selective reflection-spectra obtained with pump intensity 255 mW/cm^2 are presented in Fig. 11: all spectra were recorded in the same experimental conditions, only the pump detuning Δ_p has been changed. Depending on this detuning, all three resonances described in the theoretical part have been observed: (i) a SVS resonance centered at detuning $\Delta_s = -(k_s/k_p)\Delta_p$, and that appears only for $\Delta_p > 0$, (ii) a resonance at $\Delta_s = 0$, which is seen experimentally for $\Delta_p \cong 0$ and for not large negative Δ_p, and (iii) a DTP resonance at $\Delta_s = -\Delta_p$, observable only when $\Delta_p < 0$. The amplitudes of the SVS resonance and the DTP resonance were comparable only for low values of Δ_p ($|\Delta_p| < 30$ MHz). At higher values of $|\Delta_p|$, the ratio of the DTP resonance amplitude to the SVS resonance amplitude is decreasing with the increase of Δ_p. The experimentally measured ratio between the DTP resonance amplitude and the amplitude of the "$\Delta_s = 0$" resonance is about 40–60, and, according to the theory, this corresponds to a ratio $A_2/A_1 = 0.10 - 0.15$.

1. "$\Delta_s = 0$" resonance

This resonance should appear whatever the Δ_p value may be, and its shape has a dispersionlike form. Since its amplitude drops quickly with increasing Δ_p, we were able to record its shape only for not large negative Δ_p ($|\Delta_p| < 30$ MHz) and even then its amplitude was close to the noise level. For positive Δ_p, this resonance is masked by the blue wing of the SVS resonance. At $\Delta_p \cong 0$, it looks more like an absorption line shape, with dips in both wings. The linewidth (distance between minimum and maximum for $\Delta_p \neq 0$) was measured to be 18 MHz, which is consistent with expected pressure broadening for the temperature inside the cell 145 °C [14]. The theory indicates that the resonance linewidth is essentially A_1 (with a small correction depending on A_2). This yields an effective value of $A_1 = 18 \pm 2$ MHz. This value of A_1 was used for the calculation of the theoretical shift of the DTP resonance. The difference between this experimental value of A_1 and the 5.3-MHz radiative-linewidth should be attributed to pressure, power, and angular broadening factors [6].

2. Stepwise velocity-selective resonance

This SVS resonance is observed when $\Delta_p > 0$. Its position and shape are in agreement with the predictions from the theoretical part. This resonance originates in the atoms ve-
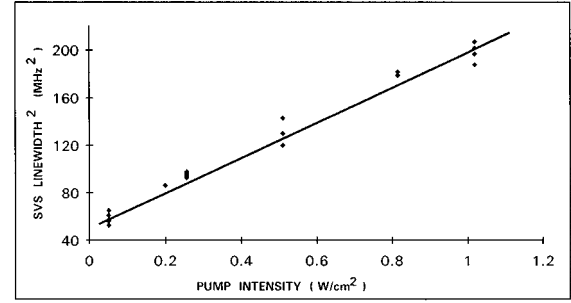
FIG. 12. Square of the linewidth (i.e., separation between the two minima) of the SVS resonance plotted against the pump intensity. Solid line is the linear fit.

locity selected by the frequency-fixed pump beam (in the counterpropagating geometry, the pump beam is resonant with atoms arriving onto the surface). Its peak-to-peak amplitude is proportional to the atomic density in the velocity class selected by the pump beam: as was demonstrated in [6], this allows us to measure the velocity distribution of atoms arriving at the surface.

The width of the SVS resonance is increasing with the pump intensity. We obtained linear dependence for the square of the width on the pump intensity (Fig. 12). By fitting the slope with the theoretical predictions (Fig. 5), we get the effective Rabi frequency of the pump:

$$\frac{\Omega_p^2(\text{MHz}^2)}{P_p(\text{mW/cm}^2)} = 0.53 \quad (\pm 10\%). \qquad (11)$$

As an example, the spectrum shown in Fig. 11 corresponds to an effective Ω_p equal to 11.6 MHz.

As seen from Fig. 12 the "low pump power" width of the SVS resonance is about 7.4 MHz. This is about 2.5 times broader than the theoretical value (3 MHz) calculated from expression (7) with $A_1 = 18$ MHz and $A_2 = 1.8$ MHz. This broadening of the SVS resonance should be attributed to the pressure and angular broadening factors.

3. Direct two-photon excitation resonance

We observed this resonance for negative pump frequency detuning at position $\Delta_s = -\Delta_p$. The amplitude of this peak is lower in comparison with the SVS resonance. According to the theory, its amplitude should decrease as $1/\Delta_p^2$ for large Δ_p. The experimental dependence of the amplitude of the DTP resonance on the pump detuning is shown in Fig. 13. The experimentally measured dependence of the width of this two-photon reflection peak, on the pump power and the pump frequency detuning, is consistent with the theoretical predictions. Within the experimental error, the width is constant.

The experimentally measured asymmetry of DTP resonance (positive to the negative part) for large negative values of Δ_p is in the range 0.7–0.8. We know from the theory that this asymmetry is very sensitive to the ratio of A_2/A_1. The experimentally measured asymmetry corresponds to the values of A_2/A_1 less than 0.1. But taking into account that the total decay rate of the $8S$ level is 1.8 MHz we accepted as
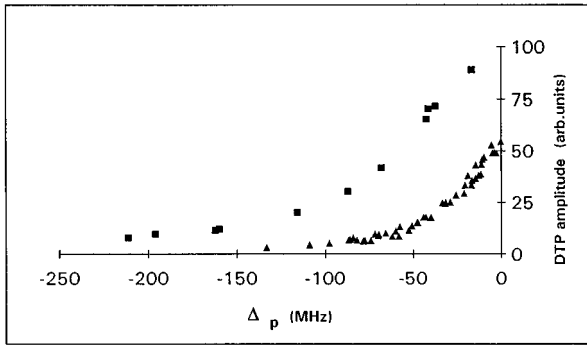
FIG. 13. Amplitude of the DTP resonance as a function of the pump detuning for two different values of the pump intensity: filled squares: 1.02 W/cm^2 pump intensity; filled triangles: 0.25 W/cm^2.

reasonable $A_2/A_1=0.1$ for the calculation of the theoretical graphs.

This experimental observation of the DTP resonance shows that this resonance can be well discriminated (amplitude linewidth) and is greatly improved in comparison with the first detection of the DTP resonance reported in [7]. Two main factors contributed to this improvement: (a) the use of pump frequency modulation instead of pump amplitude modulation, and (b) the ratio $k_s/|k_p|$ for the investigated cascade system is closer to 1:0.93 instead of 0.73, for the impact of this parameter see Fig. 8.

C. Two-photon dynamic Stark shift

The good quality of the DTP resonance allowed us to investigate the dynamic Stark shift that it experiences at high values of the pump intensity. The spectra were treated with a specially designed computer program that analyzes the reference spectra obtained from the pump and probe frequency control setups and the selective reflection spectrum. From these spectra, the program calculates the frequency scale and determines pump and probe frequency detunings Δ_p and Δ_s, and then the position of the extrema, the peak-to-peak amplitude, the asymmetry, and the width of the DTP resonance. The light shift is calculated as a spectral distance between the middle point of the DTP resonance dispersive curve and the absolute value of pump frequency deviation $|\Delta_p|$.

In Fig. 14 are shown the selective reflection spectra ob-
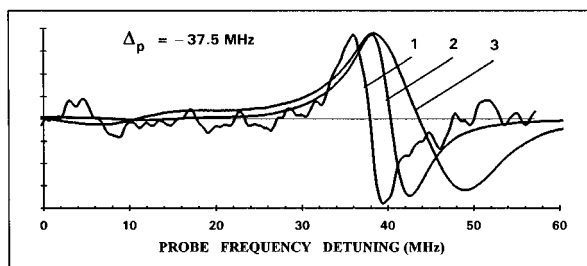
FIG. 14. DTP selective reflection spectra for three different values of the pump intensity: (1) $P_p=10$ mW (unfocused), (2) $P_p=200$ mW (unfocused), (3) $P_p=130$ mW with 1-m focusing lens. The amplitudes of the spectra are normalized to the same value.
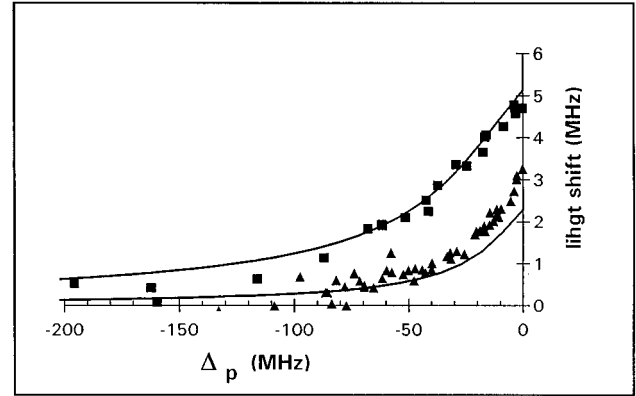
FIG. 15. Comparison between the experimentally observed and the predicted light shift of the DTP selective reflection resonance for two different values of the pump intensity. Filled squares: 1.02 W/cm^2 pump intensity, filled triangles: 0.25 W/cm^2. The most important parameter for the theoretical curves was the calculated effective Ω_p for these two intensities (see the text).

tained for pump frequency detuning -37.5 MHz and three different values of the pump power. The first two spectra (1,2) are monitored with a nonfocused pump beam with $P_p=10$ and 200 mW. For the third one (3) the beam with $P_p=130$ mW was focused with 1-m focal length lens. The light shifts for these DTP resonance spectra are 0.3, 2.9, and 6.7 MHz. With focused 130-mW pump beam and smaller values of Δ_p, the light shift is 9 MHz. The broadening of the DTP resonances in the latter case is the result of the spatial averaging of the light shift, due to the fact that the pump beam diameter is less than the diameter of the probe beam.

The dependence of the pump-induced light shift on the deviation Δ_p is shown in Fig. 15 for two different values of the pump intensities 0.25 and 1.02 W/cm^2. No focusing has been used in these measurements. The theoretical curves have been obtained with the analytical formula using values for Ω_p that are equal to 11.65 and 23.3 MHz, respectively, as estimated from the width of the SVS resonance, relation (11). No fitting parameters have been used. Some deviation exists between the theoretical curve and the experimental points for 0.25 W/cm^2 pump intensity for low values of Δ_p. An even bigger discrepancy is observed for data obtained with a pump intensity 0.05 W/cm^2. This difference between the experimental shift and the theoretical predicted shift could be attributed to two phenomena not taken into account in the theory: (i) probe saturation, which could induce an additional shift, and (ii) surface effects—for instance, the van der Waals potential acting on upper atomic states: the slow atoms responsible for the DTP resonance must be very sensitive to them.

IV. CONCLUSION

Three-level reflection spectroscopy in the pump frequency modulation mode has allowed us to single out Doppler-free two-photon reflection resonance. Pump saturation effects have been investigated. A two-photon light shift larger than the resonance width has been observed in cesium, and its power and detuning dependence have been fully interpreted in the framework of a nonperturbative theoretical approach.

Up to now, experimental study has been limited to the pump-probe counterpropagating geometry. Work is now in progress to investigate the copropagating geometry, in which the two-photon signal should be more sensitive to departing atoms. Also, the extension of the theoretical approach to include atom-surface van der Waals interactions is under way.

APPENDIX: ANALYTICAL FORMULA IN DOPPLER LIMIT APPROXIMATION AND PUMP FREQUENCY MODULATION MODE

Integration over velocity can be carried out analytically in the Doppler limit, i.e., under the assumption A_1, A_2, $|\Delta_p|$, and $|\Delta_s| \ll k v_0$. In Doppler limit the two integrals $J_+ + J_-$ can be presented as $J_\pm = (1/k_s A_1^3) \tilde{J}_\pm$ with

$$\tilde{J}_\pm = \int_0^\infty dx \left[(a_2 - i\tilde{\Delta} - ixs_\pm)(\tfrac{1}{2} - i\tilde{\Delta}_s - ix) + \frac{\tilde{\Omega}_p^2}{4} \right]^{-2},$$
(A1)

where $a_2 = A_2/2A_1$, $\tilde{\Delta}_s = \Delta_s/A_1$, $\tilde{\Delta} = \Delta/A_1$, $\tilde{\Omega}_p = \Omega_p/A_1$, and $x = k_s v/A_1$. After integration,

$$\tilde{J}_\pm = (b_\pm - c_\pm)^{-2} \left[\left(\frac{1}{b_\pm} + \frac{1}{c_\pm} \right) - 2(b_\pm - c_\pm)^{-1} \ln\left(\frac{b_\pm}{c_\pm} \right) \right],$$
(A2)

where $b_\pm$ and $c_\pm$ are the roots of the denominator of (A1):

$$b_\pm = \frac{1}{2} \left[\tilde{\Delta}_s + \frac{i}{2} + (\tilde{\Delta} + ia_2)s_\pm \right]$$
$$- \frac{1}{2} \sqrt{ \left[\tilde{\Delta}_s + \frac{i}{2} - (\tilde{\Delta} + ia_2)s_\pm \right]^2 + \tilde{\Omega}_p^2 s_\pm} \quad \text{(A3)}$$

and

$$c_\pm = \frac{1}{2} \left[\tilde{\Delta}_s + \frac{i}{2} + (\tilde{\Delta} + ia_2)s_\pm \right]$$
$$+ \frac{1}{2} \sqrt{ \left[\tilde{\Delta}_s + \frac{i}{2} - (\tilde{\Delta} + ia_2)s_\pm \right]^2 + \tilde{\Omega}_p^2 s_\pm}. \quad \text{(A4)}$$

The expressions (A3) and (A4) include the square root of complex quantity. The sign of the square roots is determined by continuity from the limit $\Omega_p \to 0$. The expression for $\Omega_p \ll A_2, A_1$ can be obtained, for example, from the Appendix of [5], by frequency derivation of expression (A4).

The final result in the Doppler limit is given by

$$I_{\text{DL}} = -B \frac{4n(n-1)}{(n+1)^3} \frac{N\hbar c \Omega_s^2 \Omega_p^2}{32\sqrt{\pi}} \frac{1}{k_s v_0 A_1^3} \text{Re}(\tilde{J}_+ + \tilde{J}_-).$$
(A5)

The analytical formula (A5) describes correctly the two-photon selective reflection spectra and pump saturation effects in pump frequency modulation mode. The main advantage of this formula is the possibility to study the role of the transversal structure of the beam. When the pump beam has Gaussian spatial distribution the splitting of the two-photon stepwise resonance is washed out and is seen as broadening of the peak. The frequency shift of the two-photon coherent peak is less than in the case of use of plane waves.

[1] R. W. Wood, Philos. Mag. **18**, 187 (1909).

[2] J. L. Cojan, Ann. Phys. (Paris) **9**, 385 (1954); J. P. Woerdman and M. Schuurmans, Opt. Commun. **14**, 248 (1975); A. M. Akul'shin, V. L. Velichanskii, A. S. Zibrov, V. V. Nikitin, V. A. Sautenkov, E. K. Yurkin, and N. V. Senkov, Pis'ma Zh. Eksp. Teor. Fiz. **36**, 247 (1982) [JETP Lett. **36**, 303 (1982)]; M. Oria, D. Bloch, and M. Ducloy, in *Laser Spectroscopy IX*, edited by M. S. Feld *et al.* (Academic, New York, 1989), pp. 51–53.

[3] M. Oria, M. Chevrollier, D. Bloch, M. Fichet, and M. Ducloy, Europhys. Lett. **14**, 527 (1991); M. Chevrollier, D. Bloch, G. Rahmat, and M. Ducloy, Opt. Lett. **16**, 1879 (1991); M. Chevrollier, M. Fichet, M. Oria, G. Rahmat, D. Bloch, and M. Ducloy, J. Phys. (France) II **2**, 631 (1992).

[4] M. Ducloy and M. Fichet, J. Phys. (France) II **1**, 1429 (1991).

[5] F. Schuller, O. Gorceix, and M. Ducloy, Phys. Rev. A **47**, 519 (1993).

[6] O. A. Rabi, A. Amy-Klein, S. Saltiel, and M. Ducloy, Europhys. Lett. **25**, 579 (1994).

[7] A. Amy-Klein, S. Saltiel, O. Rabi, and M. Ducloy, Phys. Rev. A **52**, 3101 (1995).

[8] I. M. Beterov and V.-P. Chebotaev, in *Progress in Quantum Electronics*, edited by J. H. Sanders and S. Stenholm (Pergamon, Oxford, 1977), Vol. 3. and references therein; M. Ducloy, J. R. R. Leite, and M. S. Feld, Phys. Rev. A **17**, 623 (1977).

[9] M. Ducloy, Opt. Lett. **7**, 432 (1982); G. Camy, Ch. Bordé, and M. Ducloy, Opt. Commun. **41**, 325 (1982).

[10] B. Cagnac, G. Grynberg, and F. Biraben, J. Phys. (Paris) **34**, 845 (1973).

[11] C. E. Theodosiou, Phys. Rev. A **30**, 2881 (1984).

[12] B. Dahmani, L. Hollberg, and R. Drullinger, Opt. Lett. **12**, 876 (1987).

[13] W. Vassen, Claus Zimmermann, R. Lallenbach, and T. Hänsch, Opt. Commun. **75**, 435 (1990).

[14] N. Papageorgiou, M. Fichet, V. Sautenkov, D. Bloch, and M. Ducloy, Laser Phys. **4**, 392 (1994).